Preparation of Multiphase Poly(Styrene-co-Butyl acrylate)/Wax-Clay Nanocomposites via Miniemulsion Polymerization

Nagi Greesh[1], Adriaan S Luyt[2]

[1]Advanced laboratory for chemical analysis, Libyan Authority to Research , Science and Technology., Tajora, Tripoli, Libya
[2]Center for Advanced Materials, Qatar University, PO Box 2713, Doha, Qatar

Abstract— *In the presence of different wax-clay nanocomposites concentrations, poly(styrene-co-butyl acrylate) P(S-co-BA) copolymers were prepared via free-radical random copolymerization of styrene and butyl acrylate in miniemulsion. Wax-clay nanocomposites were obtained through ultrasonic mixing at a temperature above the melting point of the wax at different clay loadings (1, 5, 7 and 10 wt%). The main objectives of this study were to obtain a good exfoliation of the clay platelets in the paraffin wax. The obtained wax-clay nanocomposites were then used as filler in the preparation of P(S-co-BA)/wax-clay nanocomposites via miniemulsion polymerization. X-ray diffraction (XRD) and transmission electron microscopy (TEM) indicated that the clay platelets were mostly exfoliated in the paraffin wax at low concentrations, and partially exfoliated at high concentrations. The particles morphology of the P(S-co-BA)/wax-clay nanocomposite latexes was mainly determined by TEM, and the wax-clay nanocomposites were found to be encapsulated inside the P(S-co-BA) particles and that core/shell morphology was obtained. The morphology of the P(S-co-BA)/wax-clay nanocomposites (after film formation) ranged from exfoliated to intercalated structures, depending on the percentage of wax-clay nanocomposites loading. The impact of the wax-clay loading on the thermal stability and the thermo-mechanical properties of the final polymer wax-clay nanocomposites were determined.*

Keywords— paraffin wax-clay, poly(styrene-co-butyl acrylate), nanocomposites, encapsulation, miniemulsion, core/shell

I. INTRODUCTION

Indeed, polymer/clay nanocomposites PCNs have been the topic of many research for decades, because PCN materials exhibit excellent mechanical, thermal, and gas barrier properties relative to the corresponding neat polymers.1-4 PCNs have been classified into three major classes: conventional composite, the polymer chains have failed to penetrate the clay galleries during the PCN synthesis and the clay particles exist as agglomerates within the polymer matrix; intercalated nanocomposites, where the interlayer spacing of the clay layer is expanded by polymer insertion, although the lamellar order of the clay is still maintained; and exfoliated nanocomposites, this type of structure can be formed when all individual clay layers are fully separated from each other, and are no longer close enough to interact with one another. 4-6 The incorporation of clay layers into polymers via different process such as exfoliation adsorption, template synthesis, melt intercalation, and in situ intercalative polymerization has been extensively studied. 2, 7-9 However, the dispersion of clay layers in matrices composed of smaller molecular components such as paraffin wax to produce potentially useful materials has been less studied. 10Among the few recent articles that reported on the incorporation of clay into paraffin wax, only intercalated or partially exfoliated structures have been obtained. 10 This contribution is a new attempt to obtain fully exfoliated clay layers in paraffin wax; the idea was to disperse clay in small amounts of styrene monomer in the initial stage, in order to ensure that the clay galleries become wider due to the compatibility between the styrene monomer and the organic modifier attached to the clay surface. In the second stage, molten paraffin wax was added to this dispersion and stirred for 3 h, then sonicated for 20 min. The obtained wax-clay nanocomposites were introduced into a miniemulsion process in order to obtain polymer/wax-clay nanocomposite latexes (PWCNs).

Miniemulsion is a convenient one-step technique that can be used for the incorporation of nano-layered filler materials such as clay11-14, carbon nanotubes15 and graphite16, 17, 18in polymer matrices. In the miniemulsion process, the oil phase, which consists of the monomer and the filler, can be dispersed in the water phase by a high-shear device such as a sonicator. This will lead to the formation of monomer droplets containing the filler particles, and stabilized by a surfactant, from which polymer particles will develop during the polymerization step19, 20. The miniemulsion technique greatly enhances the possibilities for the preparation of hybrid nanomaterials by encapsulating molecular compounds, liquids, or solid material. 12, 20-22 Using this technique, a wide variety of novel functional nanocomposites can be generated that are not accessible with other techniques.

This technique of polymer encapsulation is becoming more and more popular since polymer-encapsulated particles offer very interesting potential applications, such as adhesives, textiles, coatings, optics and electronics22-24. Several researchers successfully synthesized polymer encapsulated clay nanocomposites via dispersion25, emulsion[12] or miniemulsion11, 22, 24, 26 polymerization. Other researchers have reported on the encapsulation of paraffin wax using miniemulsion polymerization with core/shell morphology21. By using the core/shell concept, it is possible to prepare latex particles that consist of a hydrophobic core formed from highly hydrophobic materials such as waxes, surrounded by a less hydrophobic shell composed of relatively hydrophobic polymer(s). 21

Herein, a wax-clay nanocomposite was dispersed in water in the presence of monomers (i.e. styrene and butyl acrylate) and surfactant to form a miniemulsion. The obtained miniemulsions were then polymerized to afford PWCNs.

This work reports the first attempt to encapsulate clay platelets and paraffin wax simultaneously inside polymer particles; we believe that the synthesis of such multiphase composites particles (i.e. polymer, clay and paraffin wax) provides an opportunity to tailor properties for a range of applications such as paint coatings and adhesives. It is well known that miniemulsion polymerization has been successfully used for the preparation of core/shell particles with a hydrophobic core such as wax 21. This was done by initial dispersion of the hydrophobic component using a high shear device, and the encapsulation was achieved by polymerization including phase separation within minidroplets in an aqueous phase. The paraffin wax contained exfoliated clay layers in nanometer sizes, paraffin wax chains were adsorbed onto the clay surfaces, and the clay platelets were embedded in the wax matrix. The copolymerization of styrene and butyl acrylate in the presence of the wax-clay nanocomposites should form core/shell particles, with the polymer being the shell and the wax combined with some clay platelets being the core.

The overall aim of this work was twofold: The first objective was the exfoliation of clay layers into paraffin wax through ultrasonic mixing at a temperature above the melting point of the paraffin wax. The second objective was the copolymerization of styrene and butyl acrylate via miniemulsion polymerization in the presence of the exfoliated wax-clay nanocomposites. The impact of the wax-clay nanocomposites loading on the morphology, thermal and thermo-mechanical properties was investigated..

II. EXPERIMENTAL

Materials

Soft paraffin wax (M3 wax) was supplied in powder form by Sasol Wax. This Fischer Tropsch paraffin wax consists of approximately 99% of straight chain hydrocarbons and few branched chains. It has an average molar mass of 440 g mol-1 and a carbon distribution between C15 and C78. Its density is 0.90 g cm-3 and it has a melting point range around 40-60 °C.

Cloisite 20A, natural montmorillonite modified with a quaternary ammonium salt (dimethyl, dihydrogenated tallow, quaternary ammonium chloride) (OMMT), was obtained from Southern Clay Products. Stabilized styrene and butyl acrylate monomers were obtained from Aldrich. The stabilizers were removed from these monomers by washing three times with 3% potassium hydroxide solution and then purifying by distillation under reduced pressure at 30 °C. Sodium dodecylbenzenesulfonate (98%) (SDBS) and potassium persulphate (KPS) ($K_2S_2O_8$) were obtained from Fluka.

Preparation of wax-clay nanocomposites

Wax–clay nanocomposites were prepared by mixing the OMMT at concentrations of 1, 5, 7 and 10 wt% with molten paraffin wax. In a typical procedure, OMMT (1-10% wt relative to wax) was dispersed in 15 ml of styrene monomer and stirred at room temperature, for 24 h The molten paraffin wax was added to this dispersion and stirred for an additional 3 h at 40 °C, before sonicated for 30 min using a 750 W high-intensity ultrasonic processor (frequency 20 kHz) purchased from Cole–Parmer (Model CP 505, 500 watts), set at 100% amplitude and a pulsing setting (2s/1s on/off). The sonication was carried out in an ice bath in order to keep the temperature in the range of 60-70 °C. This was done in order to avoid wax phase separation due to crystallization during sonication. Styrene monomers were removed by drying samples at 25 ºC for 3 days. The wax-clay nanocomposites containing 5 wt% clay (W-5%-CNs) was used to prepare PWCNs in miniemulsion.

Preparation of poly(S-co-BA)\wax-clay nanocomposites

The copolymerization of styrene and butyl acrylate was carried out in a 250 ml three-neck round bottom flask equipped with a baffle stirrer, a reflux condenser, a nitrogen inlet and a rubber septum, at 75 ºC. In a typical procedure styrene monomer (8.00 g), butyl acrylate (12.00 g) and W-5%-CNs (3-10 wt% relative to monomers), were mixed with sodium bicarbonate

(used as a buffer) and an SDBS/water solution. The mixture was first stirred for 20 minutes (pre-emulsification) and then sonicated using a Cole-Parmer sonicator for 30 minutes, at 90% amplitude and a pulse rate of 2.5s. The sonication was carried out in an ice bath in order to keep the temperature in the range of 60-70 °C. This was done to avoid wax phase separation due to crystallization during sonication. After the miniemulsification, the solution was immediately transferred to a 250-ml three-neck flask and suspended in an oil bath heated to 70 °C. The miniemulsion was degassed for 30 minutes, the temperature was increased to 85 °C and the K2S2O8 initiator (0.001 g) was added. The reaction was carried out for 6 h under a nitrogen atmosphere after which it was cooled to room temperature. A typical formulation recipe for the latex synthesis is shown in Table 1.

TABLE 1
MINIEMULSION FORMULATION RECIPE FOR THE SYNTHESIS OF PWCNS

Reagents	Weight (g) relative to monomers
Styrene	8.00
Butylacrylate	2.00
SDBS	0.13
$NaHCO_3$	0.026
$K_2S_2O_8$	0.001
Water	50.00
W-5%-CNs	0.6, 1.00, 1.40, 2.00
OMMT	0.03, 0.05, 0.07, 0.1

III. CHARACTERIZATION

Transmission electron microscopy (TEM) images were obtained from a JEOL 200 instrument at an accelerating voltage of 120 kV. Prior to analysis, samples of PCNs were stained with OsO4, then embedded in epoxy resin and cured for 24 h at 60 ºC. The embedded samples were cut into slices of a nominal thickness of 100 nm, using an ultra-microtome with a diamond knife on a Reichert Ultracut S ultra microtome, at room temperature. The sections were transferred from water at room temperature onto a 300-mesh copper grid. TEM analysis was also carried out on the latex to see the particles morphology on a nanometer scale. Samples were prepared by diluting the latex in water. The diluted samples were mounted on copper grids for TEM analysis.

A Perkin-Elmer TGA7 thermogravimetric analyzer (Waltham, Massachusetts, U.S.A.) was used to investigate the degradation of the PWCNs samples. Thermogravimetric analyses were done under flowing nitrogen gas (20 ml min-1). Samples weighing between 5 and 10 mg were placed in platinum pans and analyzed from 30 to 600 °C at a 10 °C min-1 heating rate.

A Perkin-Elmer Diamond DMA (Waltham, Massachusetts, U.S.A.) was used to assess the dynamic-mechanical performance of the PWCN, samples sizes were 5mm x10mm. Temperature ramp experiments were conducted using a dual cantilever rectangular geometry with a temperature sweep from –150 to 100 °C at a 5 °C min-1 heating rate. The frequency used in the measurements was 1 Hz.

XRD results were obtained by using a Panalytical X'pert PRO PW 3040/60 X-ray diffractometer (XRD) with a CuKα (λ = 0.154 nm) monochromated radiation source collected in the range of 2θ = 0.5-30°) and steps of 0.02°. The samples were exposed to X-rays for 20 min.

IV. RESULTS AND DISCUSSION

Characterization of wax-clay nanocomposites

Figure 1 shows the XRD patterns of the commercial paraffin wax, OMMT, and the wax-clay nanocomposites at various clay loading levels (5, 7, and 10 wt %).The OMMT clay has a d- spacing of 36 nm (2θ = 3.7°).

The final morphology of the wax-clay nanocomposites prepared is undoubtedly influenced by the OMMT content. At 5 wt% OMMT loading no OMMT peak could be observed in the XRD patterns. This may be due to either the absence of periodically stacked MMT layers (i.e. an exfoliated structure was obtained) or to the detection limit of the instrument, according to Eckel at el 27 XRD cannot be used to quantify the dispersion. Dilution of the clay, preferred orientation, mixed-layering, and other peak broadening factors make XRD characterization of polymer nanocomposites susceptible to errors. The formation of a partially exfoliated structure of the wax-clay nanocomposite at 1 wt% and 5 wt% OMMT loading was

confirmed by TEM as seen in Figure 2 (A and B), the clay platelets dispersed as single layers, while others remained stacked in an orderly manner, indicating a partially exfoliated structure.

However, for the wax-clay nanocomposites prepared at high clay contents (7 wt% and 10 wt%), a peak (indicated by the arrow in Figure 1) appeared and shifted to a lower 2θ value relative to the OMMT peak. This is consistent with an intercalated clay structure into which wax molecules penetrated to separate the clay platelets. the TEM image of the wax-clay nanocomposites prepared using 7 wt% OMMT (Figure 2 (C, and D)) shows that fewer individual platelets and more clay layers were seen (Figure 2D), indicating a smaller degree of exfoliation, and a higher level of intercalation.

It is interesting to compare the morphologies of the wax-clay nanocomposites prepared in the present study with those obtained by other researchers; Wang et al. 27 prepared wax-clay nanocomposites through ultrasonic mixing at temperatures above the melting point of the wax. However, even at low clay loading, a fully exfoliated structure was never obtained. In our study the OMMT layers were first dispersed in a styrene monomer, due to the compatibility between the styrene monomer and the organic clay modifier (dimethyl, dehydrogenated tallow, quaternary ammonium chloride). This increased the d-spacing of OMMT and facilitated the migration of the molten paraffin wax molecules inside the clay galleries, which to some extent exfoliated the clay platelets in the paraffin wax matrix after sonication. At relatively high clay concentrations (such as 7 wt % and 10 wt %), the distance between the clay layers is comparable to, or even smaller than the size of a single layer of clay. This increased the frictional interactions between the OMMT layers and restricted the movements of the clay platelets, inhibiting their separation and giving a mixed morphology with a number of intercalated structures.

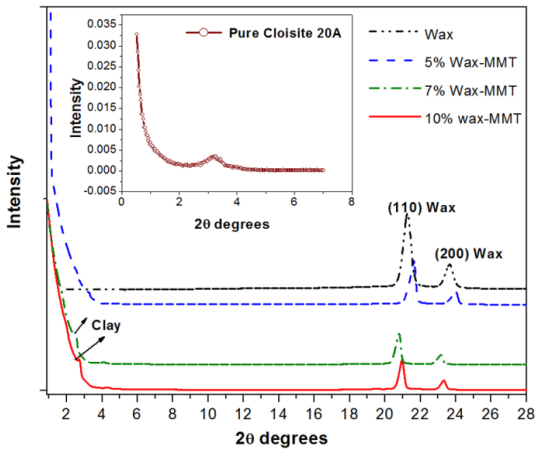

FIGURE 1: XRD PATTERNS OF THE COMMERCIAL PARAFFIN WAX, OMMT, AND THE WAX-CLAY NANOCOMPOSITES AT VARIOUS CLAY LOADING LEVELS (5, 7, AND 10 WT %)

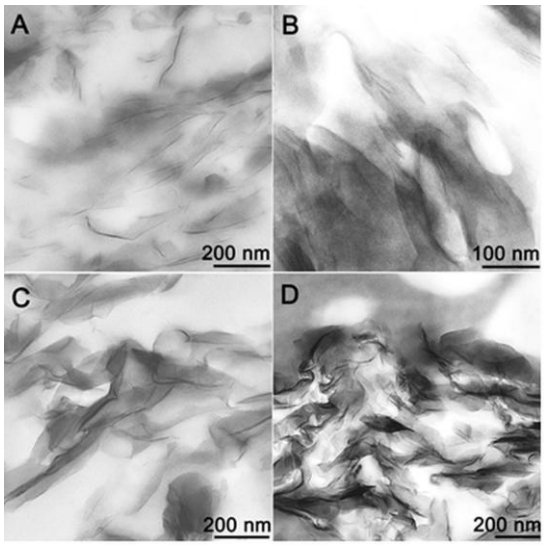

Figure 2: TEM images of wax-clay nanocomposites prepared at different clay loadings: (A) 1%, (B) 5%, (C) 7%, and (D) 10%.

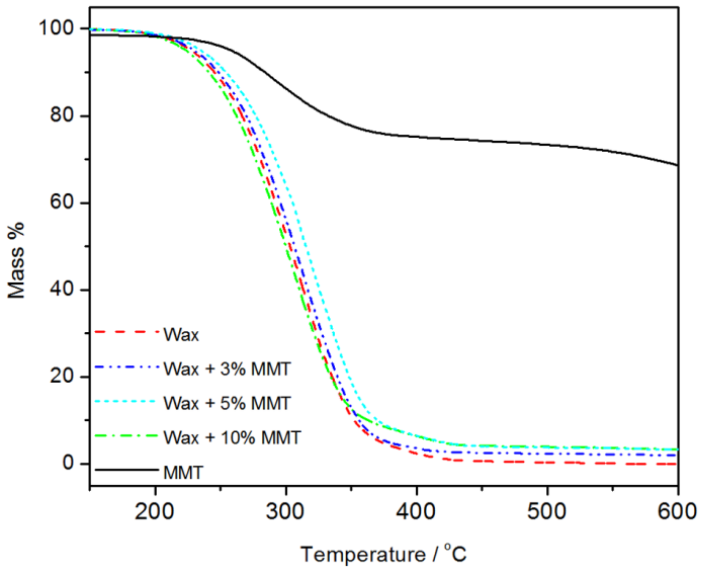

FIGURE 3: TGA CURVE OF MMT, PARAFFIN WAX, AND WAX-CLAY NANOCOMPOSITES PREPARED AT DIFFERENT CLAY LOADINGS

The decomposition behaviour of OMMT, paraffin wax, and wax-clay nanocomposites at different clay contents was examined by TGA (Figure 3). **In general all the wax-clay nanocomposites decomposed in a similar fashion. Pure paraffin wax started decomposing at 220 °C, and** its decomposition temperatures were only slightly affected by the presence of OMMT. The extent to which the thermal stability of paraffin wax was improved did not correlate linearly with the clay loading. This is because the improved thermal stability in wax-clay nanocomposites is not only due to clay loading, but is also closely dependant on other factors such as the degree of interaction between the clay and the paraffin wax, the degree of dispersion of the clay nanofiller, and the overall morphology, For instance, wax-clay nanocomposites synthesized using 10 wt% clay were found to be thermally less stable than those prepared using 3 and 5 wt% clay. The changes in thermal stability can be directly correlated with the structure of the nanocomposites (intercalated or exfoliated) and not with the amount of clay incorporated into the wax. Partially exfoliated structures with low clay loading (5 wt%) showed stronger improvements in thermal stability than those with intercalated structures (10 wt%). The homogenous dispersion of clay into the paraffin wax matrix in the partially exfoliated structures could provide a greater interfacial area between the paraffin wax chains and the clay platelets, giving higher thermal stability than for the intercalated structure, similar to the behaviour of clay in other PCNs2, 28. In the case of the exfoliated morphology there is better interaction between the wax molecules and the individual clay platelets, which may retard the onset of degradation or inhibit the diffusion of volatile degradation products out of the sample.

Particles morphology determination

Figure 4 shows the TEM images of P(S-co-BA) colloid particles prepared using different amounts of W-5%CNs. The particle size distribution was fairly narrow, which is an indication that little secondary particle nucleation occurred during the polymerization process. This was expected in our system because the wax-clay could form a physical barrier and makes it difficult for species, such as growing radicals, to be transported toward the particle surface prior to the exit into the water phase. However, as clay loading increased, a few small particles began to appear. The appearance of these secondary particles was attributed to initiator derived chains emanating from a small amount of KPS that dissolved in the aqueous phase. The images show the P(S-co-BA) particles in miniemulsion after staining with RuO4. The dark domains represent P(S-co-BA), whereas the lighter domains are attributed to paraffin wax, indicating that a core/shell morphology was obtained. These are not surprising results, because it is well known that miniemulsion polymerization has been used to prepare core/shell particle with hydrophobic cores such as hexadecane or wax 21. This was done by the initial dispersion of the hydrophobic component using a high shear device. Luo and Zhou21 confirmed that miniemulsion polymerization is a very promising technique for the encapsulation of hydrophobic compounds. They studied the nanoencapsulation of paraffin wax into poly(styrene-co-methyl methacrylate) particles using miniemulsion polymerization. In our case the paraffin wax

contained 5 wt% of OMMT, The majority of clay platelets could not be seen in the TEM images in Figure 4 a, and b, except few areas where clays are seen around the polymer particles. The absence of the clay sheets in the latex suggests that most of these clay platelets were encapsulated in the polymer particles. However, a few clay platelets were unable to enter the polymer particles and bridged the particles in the so-called linked particle formation. It is worth to mention that although almost of polymer particles have a wax-clay-core/polymer-shell structure. However, we can find three groups of particle morphologies. Some of the particles have paraffin-core/polymer-shell structures, some exhibit half-moon morphology, and the remaining particles are composed of pure polymer. The formation of the particles of pure polymer could be ascribed to homogeneous nucleation. It has been found that the presence of a hydrophilic monomer (i.e. BA) can increase the probability of homogeneous nucleation competing with droplet nucleation.21

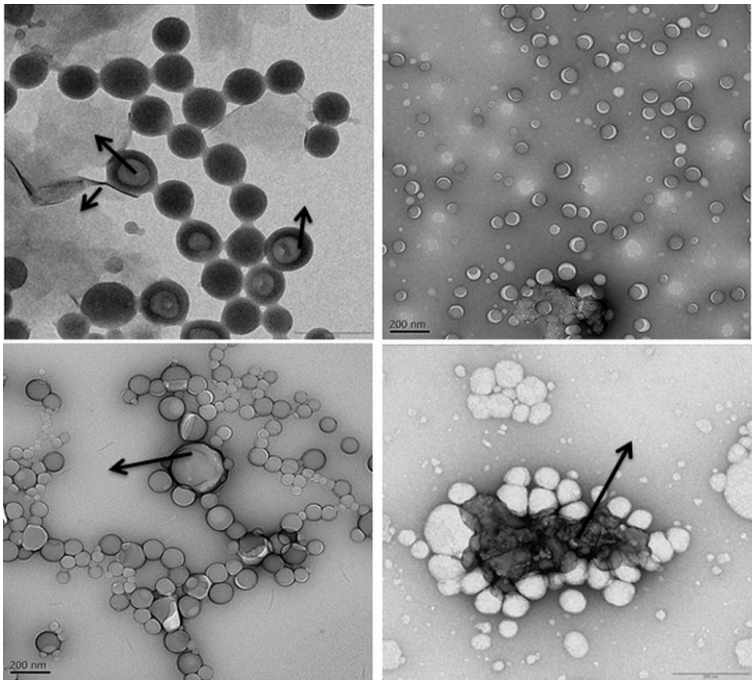

FIGURE 4: TEM IMAGES OF P(S-CO-BA)/WAX-CLAY NANOCOMPOSITES COLLOID PARTICLES CONTAINING DIFFERENT AMOUNTS OF W-5%CNS: (A) 3 WT%, (B) 5 WT%, (C) 7 WT%, AND (D) 10 WT%.

The half-moon particles observed are the fewest. It is assumed that these particles nucleate at last. Before the nucleation, some of the monomers residing in the unnucleated droplets are transported to the nucleated droplets (particles), and this increases the paraffin/monomer ratio in the droplets left behind. In the case of a high ratio of paraffin to polymer, half-moon morphology is favourable.22 Furthermore; it is possible that the polymer shell is too weak to resist the shrinkage caused by paraffin crystallization after polymerization or expansion caused by paraffin melting during TEM observations.21

In our case the clay platelets were highly hydrophobic and homogeneously distributed in the paraffin wax, and hence had a high affinity for the monomers. They were encapsulated into the growing P(S-co-BA) particles when the core/shell particles were formed during the course of the miniemulsion polymerization. The clay platelets are expected to be embedded in the wax core, giving multiphase composites particles. It is interesting to notice that, most polymer particles are not isolated but rather tend to assemble together. This could be because wax molecules are distributed on both sides of the clay surface, and two colloid particles share the same clay layers.

The inability to see the clay nanoparticles embedded into polymer particles (in the TEM images) when sample were prepared directly from the dispersion medium, has commonly been reported.23, 25, 26, 29 However, it is still possible to monitor the PWCNs morphology by viewing the clay dispersion state, after film formation, from thin slices of epoxy resin embedded pre-casted films.

As seen in Figure 4, some particles were deformed, which could be due to the high vacuum conditions used in TEM. It is also interesting to note that on the TEM images, most particles are not isolated but rather tend to assemble together. This could be because the paraffin wax was distributed on both sides of the clay surface, and the two colloid particles shared the

same clay layers. As wax-clay nanocomposites loading increased (10 wt%) there no core/shell morphology could be seen and the aggregation of clay layers was clearly observed (Figure 4D), this is due to viscosity increases, which in agreement with Cho and Lee 30 who found that the diffusional resistance, which is related to the chain mobility, plays an important role in the rate of morphological change of particles during polymerization, and the key factor is the viscosity in the polymerization process. In our case the viscosity of the reaction medium substantially increased with montmorillonite clay loading, and therefore the high viscosity in the polymerization locus probably decreased the degree of phase separation by creating a kinetic barrier for polymer chain diffusion and the wax-clay remained aggregated in the water phase.

The lager amount of wax-clay will result in more aggregates of wax-clay. This aggregated wax-clay will not be able to enter the particles, so they will be distributed around the polymer particles. The polymer particles tend to link together to house the wax-clay as shown in figure 4 D.

Morphology of P(S-co-BA)/wax-clay nanocomposites

The techniques most commonly used for characterization of clay nanocomposite morphologies are TEM and XRD.31, 32 TEM is an excellent qualitative analytical technique to monitor the extent of clay dispersion in a polymer matrix. Dry films of the PCNs material were prepared by removal of the dispersion phase, followed by drying the obtained powder at 120 ºC for 24 h. Figure 5 shows the TEM images of P(S-co-BA)/wax-clay nanocomposites containing different W-5%CNs loadings.

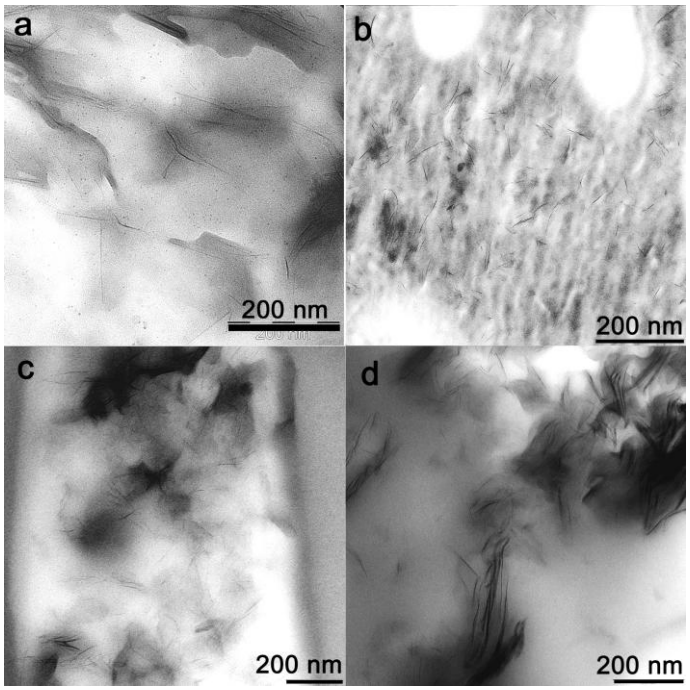

FIGURE 5: TEM IMAGES OF P(S-CO-BA)/WAX-CLAY NANOCOMPOSITES CONTAINING DIFFERENT AMOUNTS OF W-5%CNS (A) 3WT%, (B) 5WT%, (C) 7WT% AND (D) 10WT%.

Contrary to the TEM images shown in Figure 4, where the majority of clay platelets were not visible, Figure 5 (a and b) demonstrates that the clay particles were indeed embedded inside the P(S-co-BA) particles during the miniemulsion polymerization. Some clay layers were still found closely packed and appear as dark lines, while some individual clay layers were well distributed in the polymer matrix, which is typical of partially exfoliated structures. As the clay loading increased, the silicate layers came closer to each other and intercalated nanocomposites were obtained as seen in Figure 5 (c and d), indicating that the PWCNs structure is strongly dependent on the wax-clay/polymer ratio. These results are consistent with those of other researchers who obtained exfoliated structures in emulsion polymerization at low clay loading, and intercalated structures at high clay loading 33-35.

The XRD patterns of the PWCNs are shown in Figure 6. The two sharp peaks (A and B) are related to the paraffin wax36, while the broad peaks (C and D) are related to the lamellar structure of P(S-co-BA). The lamellae are believed to be due to the self assembly of paraffin wax and SDBS in the presence of P(S-co-BA). Previous literature reported that the self

assembly of SDBS and wax can both form lamellar structures 37, 38. The XRD patterns shown here are similar to those obtained by Moraes et al.39 who prepared P(S-co-BA)-clay nanocomposites via miniemulsion polymerization. However, they did not well explain their XRD results.

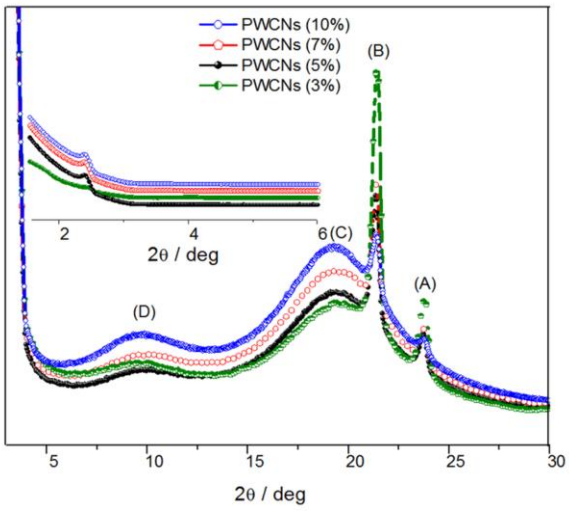

FIGURE 6: XRD FOR P(S-CO-BA)/WAX-CLAY NANOCOMPOSITES CONTAINING DIFFERENT AMOUNTS OF W-5%CNS.

Of particular interest is the peak at the 2θ = 2.3 (insert in Figure 6), which is related to OMMT. At higher wax-clay loadings (≥ 5 wt%) the peak is well defined and shifted to lower 2θ values relative to that of pure OMMT, indicating that an intercalated morphology was obtained, consistent with the TEM results. The OMMT peak is, however, not distinguishable at low wax-clay nanocomposites levels, which is due to either a loss of order (exfoliation) or the low concentration of clay in the polymer matrix. However, TEM imaging seems to favour the semi-exfoliation hypothesis, as only few regularly oriented clay particles were observed.

Thermal stability

The thermal stability of the P(S-co-BA)/wax-clay nanocomposites and the pure copolymer were studied by TGA. Figure 7(a) shows the TGA curves, and Table 2 shows the temperatures at various mass % values during the thermal decomposition. All the TGA curves show a single mass loss step. Furthermore, all the PWCNs were found to be thermally more stable than the neat copolymer prepared under similar conditions. Figure 7(b) shows the TGA curves of copolymers prepared using 10 wt% of W-5%CNs, and in the absence of OMMT (i.e. only with 10% wax).

TABLE 2
TGA DATA FOR PWCNS AT VARIOUS WAX-5%CNS LOADINGS

Wax-5%CNs (Feed) (wt%)	$^{*}T_{10\%}$ / °C	$^{**}T_{50\%}$ / °C	% Clay	Theoretical clay percentage
0	339	376	0.00	0.00
10% wax	301	388	0.00	
3	330	380	0.28	0.00
5	341	387	0.68	
7	357	388	0.68	0.15
10	363	388	0.95	

T10%,T50% and % clay: temperatures at which 10% weight loss and 50% weight loss occurred, and experimental % clay as determined from the remaining char weight at 600 ºC*

The improvement in thermal stability of polymers filled with nanoclay is generally attributed to the formation of a clay char that acts as a mass transport barrier and a thermal insulator between the bulk polymer and the surface where the combustion takes place 2, 40. It has also been suggested that delaminated clay sheets may hinder the diffusion of volatile decomposition products within the nanocomposite materials 2, 4, 28. In addition, restricted thermal motion of polymer chains localized inside the clay galleries also promotes enhancement of thermal stability of PCNs 28, 41. On the other hand, it is known that the thermal stability of polymer-wax blends decreases with an increase in wax content as a consequence of the lower thermal stability of the wax 42, 43. The TGA results in Figure 7 show that the decomposition temperatures of the copolymer were

observably affected by the W-5%CNs content. P(S-co-BA)/wax-clay nanocomposites with 10 wt% and 7 wt% of W-5%CNs showed a large increase (± 20 ºC) in the onset temperature of degradation, compared to that of the neat copolymer. In addition, the temperature at which 50% degradation occurred increased with up to 15 ºC. PWCNs prepared using 3 wt% and 5 wt % of W-5%CNs loading also showed an improvement in thermal stability, but to a smaller extent. The thermal stabilities of the PWCNs prepared in this study were clearly affected by the presence of OMMT, although the concentrations of OMMT were very small relative to the amount of paraffin wax. This is in agreement with literature which shows that even low clay loadings can provide improvement in thermal stability 5, 31, 44. For example, Doh and Choi[44] report that the maximum thermal stability of polystyrene/clay nanocomposites is reached when only 0.3% clay is used. It is known that the thermal stability of nanocomposites depend on several factors such as the filler type, filler loading 45, and nanocomposite morphology 7 (i.e. the degree of filler distribution in the polymer matrix). The results obtained in our study show that the clay loading seems to be the main factor affecting the thermal stability of the PWCNs.

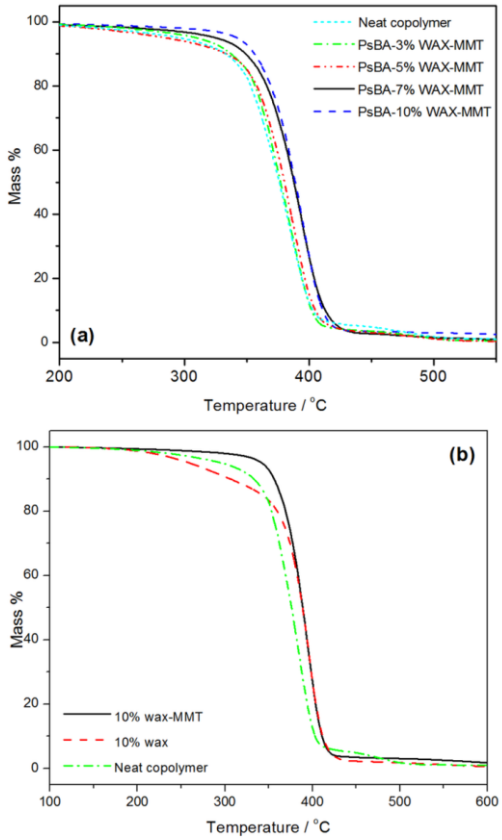

FIGURE 7: (A) TGA CURVES OF PWCNS PREPARED WITH DIFFERENT WAX-5%CNS LOADING AND (B) COMPARISON OF THE THERMAL STABILITY OF COPOLYMERS PREPARED USING 10 WT% WAX-5%CNS AND 10 WT% PURE WAX. THE TGA CURVE OF THE NEAT COPOLYMER IS INCLUDED AS A REFERENCE.

The copolymer prepared using only 10 wt% paraffin wax shows a decrease in the onset temperature of degradation (± 40 °C) as seen in Figure 7b. This was expected since the paraffin wax is clearly less thermally stable than the neat copolymer, with almost a 90 °C difference between their respective onset temperatures of degradation. Surprisingly, the polymer-wax (with 10 wt% paraffin wax) sample shows a shift in the temperature, at which 50% degradation occurred, to higher temperatures compared to the pure copolymer. Similar results were obtained by Mpanza et al.46 who prepared low-density polyethylene through melt blending in a Brabender mixer. They found that the blends show a shift in the onset of decomposition to higher temperatures compared to the pure materials, and they interpreted their results as follows: Since thermal degradation starts at the weak bonds or chain ends, it is possible that the less thermally stable wax chains are somehow protected in the thicker PE lamellae. At the same time, the wax chains improve the stability of the PE by increasing its crystallinity. The reasons for this behaviour in our are still unclear, although it is likely due to the formation of a lamellar structure, as confirmed by XRD in Figure 6.

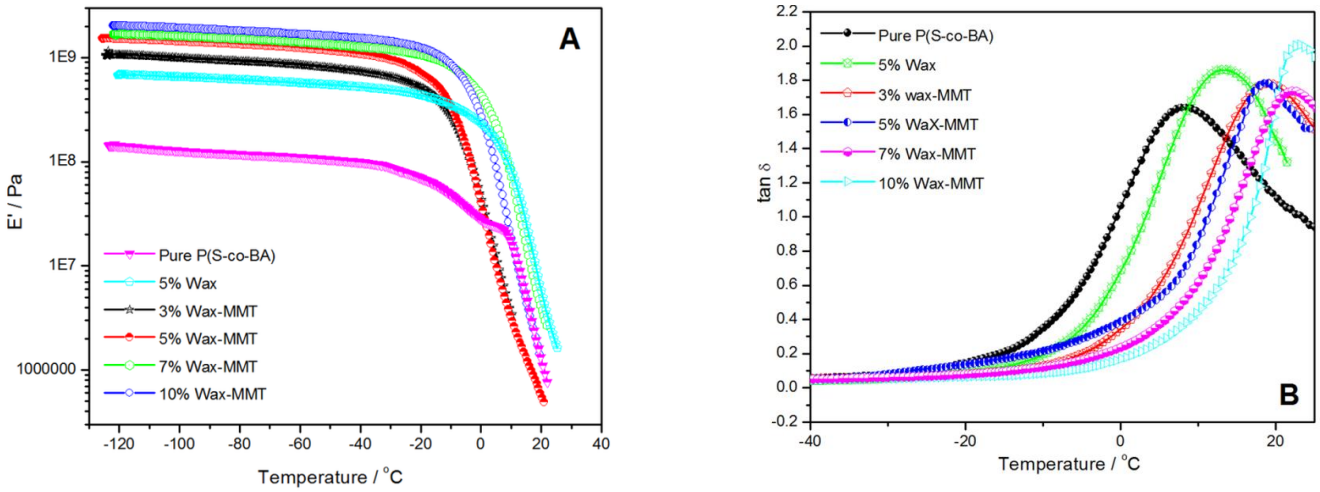

FIGURE 8: VARIATION OF (A) STORAGE MODULUS AND (B) TAN Δ VERSUS TEMPERATURE FOR PURE P(S-CO-BA) AND PWCNS PREPARED USING DIFFERENT WAX-CLAY NANOCOMPOSITES CONCENTRATIONS. (WAX-MMT IS WAX-CLAY NANOCOMPOSITES).

The copolymer prepared using 10 wt% wax-clay nanocomposites did not undergo any decrease in the onset temperature of degradation, although 10 wt% of paraffin wax was added. This can be attributed to the intercalation of paraffin wax molecules into the clay galleries. The paraffin wax chains would have been trapped between the clay nanosheets, which probably acted act as an insulator between the heat source and the paraffin wax.

Table 2 and Figure 7 show that the percentage of clay (determined from the %Char at 600 ºC) was slightly higher than the theoretical clay percentage. Initially it was expected that the %Char at 600 °C would be close to the initial clay percentage. This unexpected result is due to the either incomplete conversion of monomer during the polymerization, the conversion at the end of polymerization was found to be between 65–70%, giving an experimental clay content that is slightly higher than expected. The presence of wax-clay particles in the polymerization system, which impeded the diffusion of the initiator and monomers can affect the monomer convarsion, wax-clay particles can also hinder the growth of polymer chains during polymerization, which also leads to a inhibited in monomer conversion.

Dynamic mechanical properties

Dynamic mechanical analysis was undertaken on the PWCNs samples to evaluate the effect of wax-clay nanocomposites loading on the thermo-mechanical properties. Figure 8A shows the variation in storage modulus with temperature for the pure copolymer and the PWCNs. Due to the softening effect of the wax melting inside the polymer matrix 43, the storage modules of the obtained copolymer was expected to be dramatically decreased with increasing wax concentration. However, the storage modulus of the plateau region at temperatures below the Tg slightly increased as the wax-clay loading increased. This could be due to the incorporation of the high aspect ratio particles (montmorillonite clay), which led to an increase in the storage modulus due to interactions between the polymer matrix and the surface of the silicate layers of the clay nanofiller. This caused the mobility of the polymer segments near the interface to decrease, leading to improved mechanical properties in general.6, 47, 48 However, the copolymer prepared with only 5 wt% wax and in the absence of clay also shows an increase in storage modules. In this case the wax acted as a highly crystalline filler and thus immobilized the polymer chains at the crystal surface, leading to a higher modulus of the polymeric matrix. This is in agreement with finding obtained by Krupa et al 49, who prepared polyethylene/paraffin wax blends and clearly saw increases in the storage modules. The copolymer prepared using 5 wt% of Wax-5%CNs shows a larger increase in storage than that for the sample prepared with 5 wt% wax. This confirms that the OMMT has a significant effect on the thermo-mechanical properties of PWCNs. Accordingly, the incorporation of both paraffin wax and OMMT are believed to contribute to changes in the storage modulus.

The Tg of the pure copolymer and the PWCNs was determined from the maximum of the relaxation peak in the DMA tan δ curve in Figure 8B. It can be seen in Figure 8B and Table 3 that the glass transition relaxation peaks of all the PWNCs shifted to higher temperatures relative to that of the pure copolymer. This was due to the restricted chain mobility of the

polymer caused by the presence of the clay platelets. The Tg of PCNs was significantly affected by the Wax-5%CNs contents. The PWCNs with 7 wt % and 10 wt % show the largest increase in Tg (16 °C) relative to that of the neat copolymer. The reason for this is that the clay acts as a bridge between the polymer chains, thus restricting the polymer chain mobility. In order to understand if the addition of paraffin wax has a significant impact on the Tg of the copolymer, DMA was carried out for the copolymer prepared with 5 wt% paraffin wax (no clay added). The relaxation peak in the tan δ curve of the copolymer in this case also shifted to a higher temperature. The wax crystallites probably acted as physical crosslinks, restricting the mobility of the polymer chains at lower temperatures. The Tg values for the PWCNs samples was therefore affected by the presence of crystalline paraffin wax and layered silicates. Both these substances restricted the copolymer chain mobility.

TABLE 3
T_g VALUES AND STORAGE MODULES OF PWCNS

Sample	% clay	G^I x 10^9 (Pa)	T_g (ºC)
Pure P(S-co-BA)	0	0.13	8
P(S-co-BA)-5 % wax	0	0.68	13
P(S-co-BA)-5%-Wax-Clay	3	1.03	17
	5	1.55	18
	7	1.68	21
	10	2.03	24

V. CONCLUSION

An organoclay was successfully dispersed and partially exfoliated in a paraffin wax matrix using sonication. The morphology of the wax-clay nanocomposites strongly depended on the clay/wax ratio. Semi-exfoliated structures were obtained at low clay loadings and changed intercalated structures at higher clay loadings. The wax-clay nanocomposites were used to prepare a water-based polymer in miniemulsion polymerization, and latex particles of P(S-co-BA)/wax-clay nanocomposites with a core/shell morphology were obtained. The core of the particles was mainly wax-clay nanocomposites, while the shell was formed by the poly(styrene-co-butyl acrylate). At high wax-clay nanocomposites loadings (around 10% wt) no core/shell morphology was obtained and aggregation of the clay layers was clearly observed. The corresponding nanocomposite cast films had an exfoliated or partially exfoliated morphology at low wax-clay nanocomposites loadings, and an intercalated morphology at higher wax-clay nanocomposites loadings.

All the PWCNs were thermally more stable than the neat copolymer, and the improvement in thermal stability was largely affected by the percentage of wax-clay loading, although the concentrations of the incorporated OMMT were very small relative to the amount of paraffin wax. Increases in the storage modulus and the Tg of the PWCNs was found and correlated with the wax-clay loading. The incorporation of both paraffin wax and OMMT are believed to contribute to changes in the storage modules and Tg.

This study highlights a new method to obtain multiphase composites particles containing hydrophobic (wax) and inorganic (clay) compounds; this will allow the preparation of PCNs materials with tailored properties for specific applications such as paint coatings and adhesives.

REFERENCES

[1] A. Panwar, V. Choudhary and D. Sharma, Journal of Reinforced Plastics and Composites 30:446 - 495 (2011).
[2] S. Ray and M. Okamoto, Progress in Polymer Science 28:1539 - 1641 (2003).
[3] A. Okada and A. Usuki, Macromolecular Materials and Engineering 291:1449 -1476 (2006).
[4] M. Alexandre and P. Dubois, Materials Science and Engineering: A 28:1- 63 (2000).
[5] H. S. Nalwa, Polymer/clay Nanocomposites, in Encyclopedia of Nanoscience and Nanotechnology. American Scientific Publishers, California, pp. 791- 843 (2004).
[6] S. Tjong, Materials Science and Engineering R 53:73 -197 (2006).
[7] N. Greesh, P. Hartmann, V. Cloete and R. Sanderson, Journal of Polymer Science Part A: Polymer Chemistry 46:3619 - 3628 (2008).
[8] R. Vaia, H. Ishii and E. P. Giannelis, Chemistry of Materials 5:1694 -1696 (1993).
[9] H. Jeon, H. Jung and S. Hudson, Polymer Bulletin 41:107 - 113 (1998).
[10] J. Wang, S. Severtson and A. Stein, Advanced Materials 18:1585 -1588 (53).

[11] C. Weiss and K. Landfester, Advanced Polymer Science 233:185-236 (2010).

[12] F. Bouanani, D. Bendedouch, P. Hemeryb and B. Bounaceur, Colloids and Surfaces A: Physicochemical and Engineering Aspects 317:751 - 755 (2008).

[13] A. Samakande, R. Sanderson and P. Hartmann, Polymer 50:42 - 49 (2009).

[14] J. Faucheu, C. Gauthier, L. Chazeau, J. Cavaille, V. Mellon and E. Bourgeat-Lami, Polymer 51:6 -17 (2010).

[15] H. Lu, B. Fei, H. Xin, H. Wang, L. Li, C. Guan and Carbon 45:936 - 942 (2007).

[16] H. Etmimi, M. Tonge and R. Sanderson, Journal of Polymer Science Part A: Polymer Chemistry 49:1621-1632 (2011).

[17] S. H. C. Man, S. C. Thickett, M. R. Whittaker and P. B. Zetterlund, Journal of Polymer Science: Part A: Polymer Chemistry 51:47 - 58 (2012).

[18] S. H. C. Man, N. Y. M. Yusof, M. R. Whittaker, S. C. Thickett and P. B. Zetterlund, Journal of Polymer Science: Part A: Polymer Chemistry 51 5153 - 5162 (2013).

[19] K. Landfester, N. Bechthold, S. Forster and M. Antonietti, Macromolecular Rapid Communinications 20:81 - 84 (1999).

[20] J. Asua, Progress in Polymer science 27:1283 -1346 (2002).

[21] Y. Luo and X. Zhou, Journal of Polymer Science: Part A: Polymer Chemistry 42:2145 -2154 (2004).

[22] K. Landfester, Angewandte Chemie International Edition 48:4488 - 4507 (2009).

[23] Z. Tong and Y. Deng, Polymer 48:4337- 4343 (2007).

[24] Q. Sun, Y. Deng and Z. L.Wang, Macromolecular Materials and Engineering 289:288 - 295 (2004).

[25] N. Greesh, R. Sanderson and P. Hartmann, Polymer International 61:834 - 843 (2012).

[26] A. Samakande, R. Sanderson and P. Hartmann, Journal of Polymer Science Part A: Polymer Chemistry 46:7114 - 7126 (2008).

[27] D. F. Eckel, M. P. Balogh, P. D. Fasulo and W. R. Rodgers, Journal of Applied Polymer Science 93:1110 - 1117 (2004).

[28] A. Leszczy´nska, J. Njuguna, K. Pielichowski and J. Banerjee, Thermochimica Acta 453 75-96 (2007).

[29] W. Wang, S. M. Howdle and D. Yanb, Chemical Communications 3939 - 3941 (2005).

[30] I. Cho and K. Lee, Journal of Applied Polymer Science 30:1903 - 1926 (1985).

[31] A. B. Morgan and J. W. Gilman, Journal of Applied Polymer Science 87:1329 -1338 (2003).

[32] V. Causin, C. Mareigo and G. Ferrara, Polymer 46:9533 - 9537 (2005).

[33] S. Qutubuddin, X. Fu and Y. Tajuddin, Polymer Bulletin 48:143 -149 (2002).

[34] P. Meneghetti and S. Qutubuddin, Langmuir 20:3424 - 3430 (2003).

[35] Y. S. Choi and I. J. Chung, Macromolecular Research 11:425 - 432 (2003).

[36] J. Wang, S. Severtson and A. Stein, Advanced Materials 18:1585 -1588 (2006).

[37] Leontidis, T. Kyprianidou-Leoudidou, W. Caser, P. Robyr, F. Krumeich and K. Kyricou, Journal of Physical Chemistry 105:4133 - 4144 (2001).

[38] V. Metivaud, A. Lefevre, L. Ventola, P. Negrier, E. Moreno, T. Calvet, D. Mondieig and M. Cuevas-Diarte, Chemistry of Materials 17:3302-3310 (2005).

[39] R. P. Moraes, A. M. Santos, P. C. Oliveira, F. C. T. Souza, M. Amaral, T. S. Valera and N. R. Demarquette, Macromolecular Symposia 245:106 - 115 (2006).

[40] J. Wang, J. Du, J. Zhu and C. A. Wilkie, Polymer Degradation and Stability 77:249 -252 (2002).

[41] A. Blumstein, Journal of Polymer Science Part A: Polymer Chemistry 3:2653 -2661 (1965).

[42] A. S. Luyt and I. Krupa, Energy Conversion and Management 50:57-61 (2009).

[43] A. S. Luyt and V. G. Geethamma, Polymer Testing 26:461 - 470 (2007).

[44] J. G. Doh and I. Cho, Polymer Bulletin 41:511 - 518 (1998).

[45] N. Greesh, P. C. Hartmann and R. D. Sanderson, Macromolecular Materials and Engineering 294 206 - 212 (2009).

[46] H. S. Mpanza and A. S. Luyt, Polymer Testing 25:436 - 442 (2006).

[47] S. Qutubuddin and X. Fu, Polymer 42:807 - 813 (2001).

[48] R. Krishnamooti, R. A.Vaia and E. P. Giannelis, Chemistry of Materials 8:1728 - 1737 (1996).

[49] I. Krupa, G. Mikova and A. S. Luyt, European Polymer Journal 43 4695 - 4705 (2007).